

Photoemission Studies of Rhodium[†]

D. T. Pierce

Laboratorium für Festkörperphysik, Hönggerberg, CH-8049, Zürich, Switzerland

and

W. E. Spicer

Stanford Electronics Laboratories, Stanford, California 94305

(Received 1 February 1971)

Photoelectron energy distribution curves from Rh at photon energies $\hbar\omega < 9$ eV exhibit peaks originating from states 0.3 and 1.05 eV below the Fermi level E_F . For $\hbar\omega > 9.0$ eV, the initial states of the peaks are functions of $\hbar\omega$. At $\hbar\omega > 10.5$ eV the two peaks have merged into a single broad peak 0.75 eV below E_F . Two other pieces of structure appear at approximately 2.4 and 3.9 eV below E_F . The results for Rh are compared to those for Pd with the help of the Pd density of states. It is found to be unlikely that the band structure of Rh can be derived from Pd through the use of a simple rigid-band model.

I. INTRODUCTION

Rhodium is one of the less well studied of the transition metals compared to, for example, Pd, which lies just to the right of Rh in the $4d$ transition-metal series of the periodic table, or compared to Ni of the $3d$ series, which lies just above Pd. Like nickel and palladium, rhodium has a face-centered-cubic (fcc) structure. Although both rhodium and palladium are paramagnetic, palladium has an increased tendency toward ferromagnetism.¹ With the exception of reflectance measurements,²⁻⁴ the experimental studies of the electronic structure of rhodium have been related to Fermi-surface properties and include measurements of the specific heat,⁵ magnetic susceptibility,⁶ and de Haas-van Alphen effect.^{7,8} Anderson⁹ has reported a relativistic-augmented-plane-wave (RAPW) calculation of the band structure and Fermi-surface properties but not of the density of state.

The photoelectron energy distribution curves (EDC's) of Rh are of general interest in our effort to understand the electronic structure of transition metals. The photoelectron spectra of Ru and Pd, the neighbors of Rh in the $4d$ transition-metal series, have been measured,^{10,11} and a comparison of the EDC's from Ru, Rh, and Pd with 8, 9, and 10 valence electrons, respectively, is of interest. The photoelectron spectra of the ferromagnetic $3d$ transition metals Fe, Co, and Ni, which are iso-electronic to Ru, Rh, and Pd are already available.¹²

II. EXPERIMENTAL PROCEDURE

The best, i. e., those containing the sharpest structure in the EDC's particularly at high energy,¹² photoemission measurements of rhodium were

obtained from thin films evaporated in high vacuum as opposed to bulk samples cleaned by argon bombardment and heating. The results presented in Sec. III are from an 800-Å-thick Rh film deposited on a quartz substrate using a Varian electron-gun evaporator. During the 20-min evaporation time the pressure increased from the base pressure of 5×10^{-11} to 1×10^{-9} Torr. A residual-gas analysis before and during evaporation indicated the presence of the same residual gases, H₂, CH₃, CH₄, CO or N₂, and CO₂. The time between film formation and measurements was short compared to the time required to form a monolayer at 5×10^{-11} . There were no changes observed during the period in which the measurements were made. Subsequent x-ray analysis indicated an fcc polycrystalline film.

The photoelectron spectra were measured with a high-resolution spherical-retarding-field energy analyzer.^{13,14} This new analyzer utilizes a screen around the emitter to form a field-free drift region. From previous measurements of Ni,^{14,15} the maximum energy error of the analyzer was estimated to be about 3% of the initial kinetic energy of the measured electrons. The photoelectron energy distributions were obtained by taking the derivative of the current-voltage curve using a previously reported ac technique.^{16,17}

A $\hbar\omega = 10.2$ -eV EDC from the 800-Å film prepared and measured in the above manner (curve A) is compared in Fig. 1 to an EDC (curve B) prepared in a poorer vacuum and measured with a cylindrical energy analyzer. The pressure during evaporation of sample B increased from a base pressure of 5×10^{-10} to 2×10^{-8} Torr. The structure in curve B is shifted slightly lower in energy compared to curve A, as expected from a lower-resolution analyzer¹³; otherwise, the results from

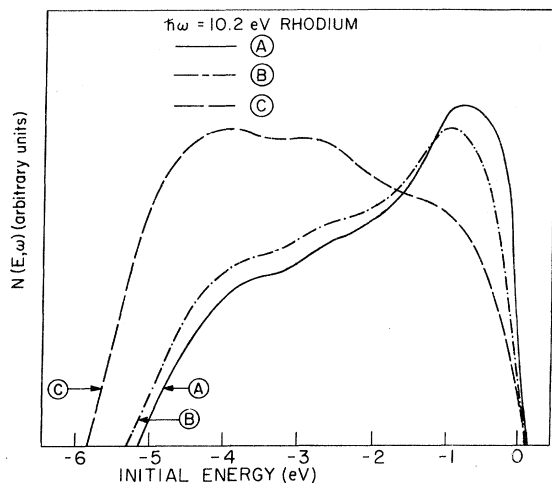


FIG. 1. EDC's at $\hbar\omega = 10.2$ eV from Rh samples prepared by (a) evaporation at 1×10^{-9} Torr, (b) evaporation at 2×10^{-8} Torr, and (c) heat and argon-bombardment cleaning.

sample B agree fairly well with sample A. Curve C in Fig. 1 is from a mechanically polished polycrystalline bulk sample which was heat cleaned for 12 h at 720°C : the base pressure was $\sim 1 \times 10^{-9}$ Torr. Subsequent argon bombardment and annealing did not significantly improve the sample. The location of structure in curve C corresponds roughly to the EDC's from evaporated films. The relatively small number of high-energy photoelectrons in curve C is typical of less clean samples, as indicated in extensive studies of nickel.¹⁵ The experience with sample C is illustrative of the difficulties encountered in preparing transition metals for photoemission measurements; at present, films evaporated in high vacuum are the most satisfactory.

III. EXPERIMENTAL RESULTS

Photoelectron spectra measured from the 800-\AA Rh film evaporated in ultrahigh vacuum are displayed in Fig. 2. The energy distribution curves were measured over the photon energy range $\hbar\omega = 6.7\text{--}11.7$ eV. The curves are plotted with respect to initial energy $E_i = E - \hbar\omega + \phi$, where the sample work function ϕ was determined to be 5.0 eV.

The EDC's for photon energies below $\hbar\omega = 8.0$ eV are characterized by a sharp peak 0.3 eV below the Fermi level. A shoulder which is partially obscured by the threshold function for $\hbar\omega < 8$ eV develops into a peak located 1.05 eV below the Fermi level in the photon energy range $\hbar\omega = 8\text{--}9$ eV. Above 9 eV the peak nearest the Fermi level has diminished to a shoulder which becomes indistinguishable from the main peak at $\hbar\omega = 10.5$

eV. The result at $\hbar\omega = 10.5$ eV of the merger of the stronger lower peak and weaker upper peak is a single broad peak 0.75 eV below the Fermi level. The peak sharpens with increasing photon energy, and moves up to 0.55 eV below the Fermi level about 11 eV. At higher photon energies there is a peak located $2.3\text{--}2.6$ eV below the Fermi level. A dip at 3.6 eV is followed by a broad shoulder or weak peak partially obscured by the escape func-

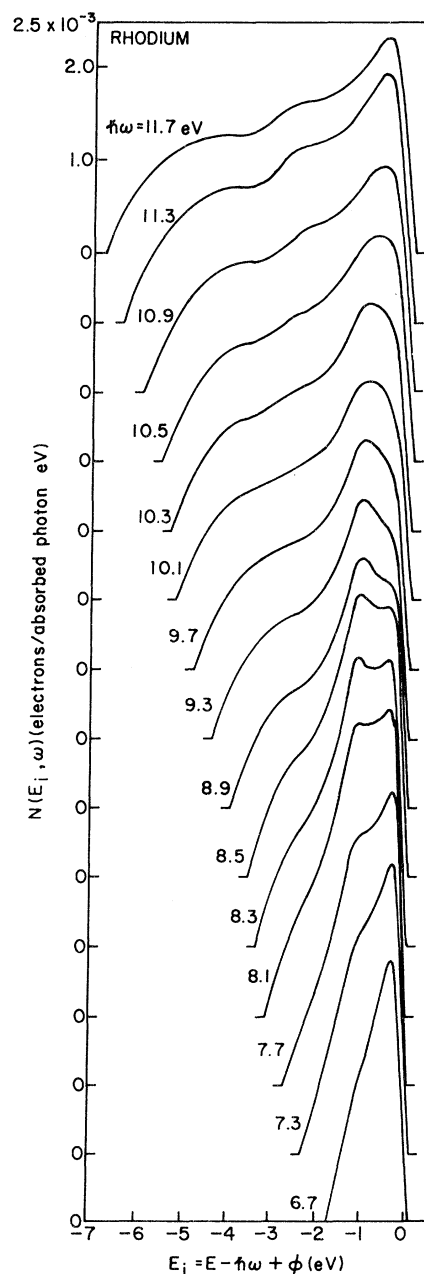


FIG. 2. EDC's from an evaporated Rh film over the photon energy range $\hbar\omega = 6.7\text{--}11.7$ eV. The curves are referred to initial-state energy $E_i = E - \hbar\omega + \phi$.

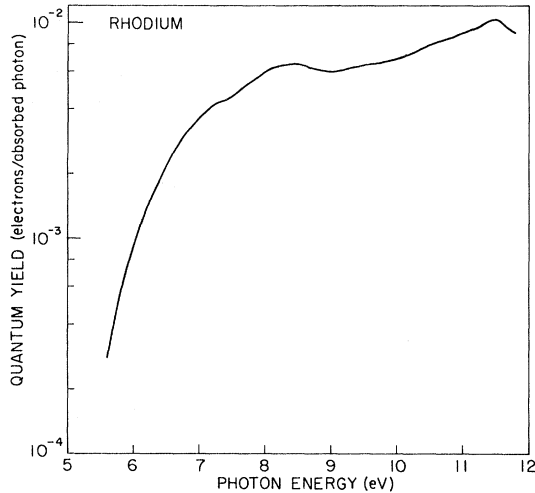


FIG. 3. The quantum yield of rhodium.

tion.

The absolute quantum yield which was used in normalizing the EDC's is shown in Fig. 3. It was measured using a calibrated Cs₃Sb photodiode, making appropriate corrections for the vacuum-chamber-window transmission and the sample reflectance.²

The change in position of the structure in the EDC's at various photon energies is summarized in Fig. 4, where the final-state energy of structure in the EDC's is plotted against the photon energy. The $E = \hbar\omega$ line is the maximum possible energy of a photoemitted electron at a given photon energy and corresponds to an electron photoemitted from the Fermi level. Therefore, at a given photon energy in Fig. 4, the initial-state energy below the Fermi level is the vertical distance below the $E = \hbar\omega$ line. A peak which originates in the same initial states at a fixed energy below the Fermi level will, in Fig. 4, be plotted along a line parallel to the $E = \hbar\omega$ line (45° from the abscissa) as the photon energy is increased.

IV. DISCUSSION

The striking feature of Figs. 2 and 4 is the way the two peaks near the Fermi level observed at lower photon energies merge into a broad peak at intermediate photon energies which narrows at higher photon energies. Such behavior is characteristic of direct transitions; that is, interband transitions between initial and final states at the same point in k space in the reduced-zone scheme. In addition, there exists the possibility that since the electron-electron scattering length decreases at a higher photon energies, electrons near the metal surface become relatively more important and distortion of the energy bands near the metal

surface might cause movement of structure in the EDC's.

In the direct-transition model, each absorbed photon is assumed to excite an electron from an initial state of energy $E_i(\vec{k})$ in band i to a final state of energy $E_f(\vec{k})$ in band f . The energy distribution of photoexcited electrons is

$$D(E, \omega) \propto \sum_{i,f} \int d\vec{k} |M|^2 \delta[E_f(\vec{k}) - E_i(\vec{k}) - \hbar\omega] \times \delta[E - E_i(\vec{k})] F_i(1 - F_f), \quad (1)$$

where $\hbar\omega$ is the photon energy, F is the Fermi function, and M is the momentum matrix element between initial and final states. The second δ function selects transitions with initial state energy E_i . If the band structure is known, it is possible to calculate the energy distribution of photoexcited electrons. Such calculations^{11,18} have been made in the constant-matrix-element approximation and have been only recently¹⁹ extended to include the interband momentum matrix elements. The energy distribution of photoemitted (instead of photoexcited) electrons can be obtained by applying appropriate threshold and escape functions.²⁰

The two lower-energy pieces of structure in Fig. 4 are seen to move out with photon energy approximately along a line parallel to the $E = \hbar\omega$ line. The scatter is largely due to the difficulty in locating this broad ill-defined structure. If these two pieces of structure are referred to initial-state energy, they remain at approximately constant positions 2.3–2.6 eV and 3.7–4.0 eV below the Fermi level. Structure behaving in this manner is typical of non-direct transitions^{20,21} (where wave vector \vec{k} is not

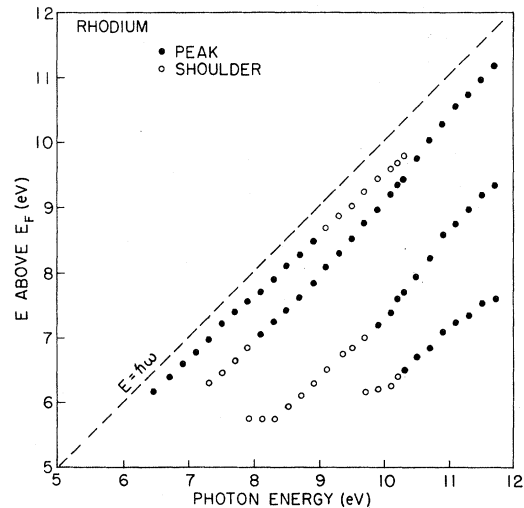


FIG. 4. Final-state energy of structure in Rh EDC's. The $E = \hbar\omega$ line is the maximum energy corresponding to an electron photoemitted from a state at the Fermi level.

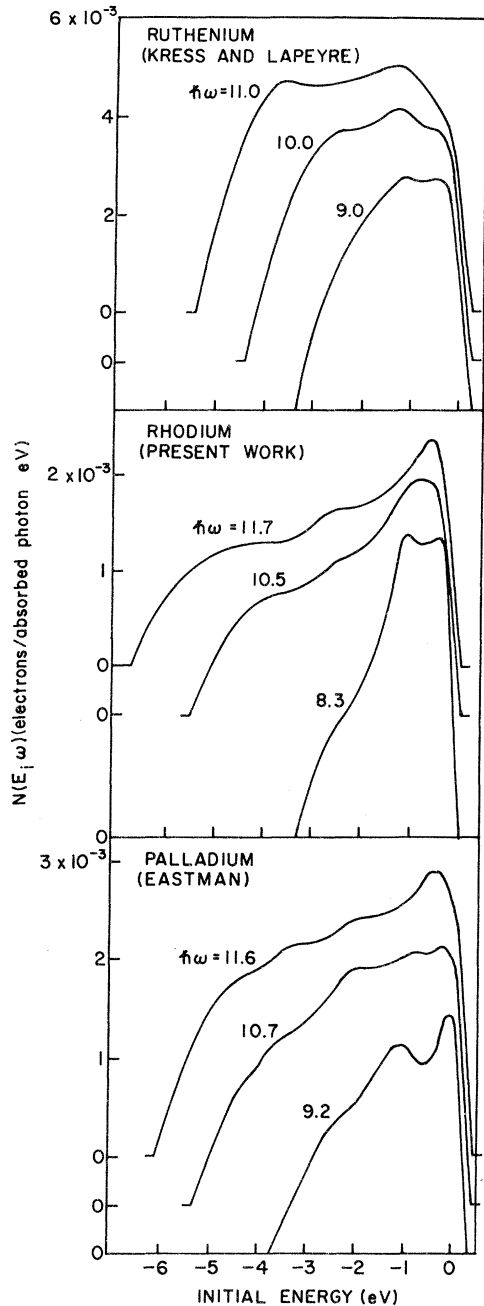


FIG. 5. Comparison of EDC's from Ru (Ref. 10), Rh, and Pd (Ref. 11).

conserved in a one-electron sense) from high initial-state density to a smooth final-state density, although direct transitions cannot be ruled out, as discussed below. In the nondirect-transition model the energy distribution of photoexcited electrons is given by

$$D(E, \omega) \propto \rho_i(E) \rho_f(E + \hbar\omega), \quad (2)$$

where $\rho_i(E)$ and $\rho_f(E + \hbar\omega)$ are the initial and final

“optical density of states.” The optical density of states may differ from the density of states obtained from a band-structure calculation because of effects of the matrix elements which have been absorbed into the optical density of states or because of many-body effects outside of the one-electron picture.²¹

We note that structure in the photoelectron spectrum which remains at a constant energy below the Fermi level when referred to initial-state energy has also been found in theoretical EDC's of Al²² and the noble metals^{18,23} calculated in the direct-transition model. In the absence of an accurate and complete band calculation from which EDC's can be calculated on a direct-transition model, it is difficult to determine if structure which lies at constant initial-state energy is likely due to direct transitions. The EDC's in Fig. 2, however, do not exhibit the strong modulation of the strength of structure which frequently occurs if the transitions are totally direct. We feel it is probable that some nondirect transitions are present in addition to the direct transitions.

A recent many-body calculation by Doniach²⁴ shows that both direct and nondirect transitions are to be expected in a *d*-band metal such as rhodium. In the case of a hole created in a narrow band, there is a strong probability of part of the photon energy going to the creation of many low-energy electron-hole pairs near the Fermi surface. In such a process, the momentum of the photoemitted electrons can undergo a large change while the energy is changed only slightly. However, Doniach's model calculation cannot be quantitatively applied to the specific case of Rh because of the complexity of the Rh band structure.

In Fig. 5 we compare representative EDC's from Ru,¹⁰ Rh, and Pd.¹¹ It is interesting to note that the double-peaked structure near the Fermi level which is most apparent in Rh near $\hbar\omega = 8.3$ eV is also apparent for Ru at $\hbar\omega = 9.0$ eV and Pd at $\hbar\omega = 9.2$ and 10.7 eV. The double peak which merges to form a broad rounded peak at $\hbar\omega = 10.5$ eV in Rh is similar to the rounded peak at $\hbar\omega = 11.6$ eV in Pd. Such behavior is not apparent in Ru but this may be because Ru has a different structure (hcp) from Rh and Pd (fcc).

The location of the major structure with respect to the Fermi level is roughly similar in the EDC's of Rh and Pd: -0.3 , -1.05 , -2.4 , and -3.9 eV in Rh and -0.15 , -1.2 , -2.2 , and 3.5 eV in Pd. Such structure in the EDC's of transition and noble metals usually corresponds to structure in the initial density of states which gives rise to the transitions, even in the case of direct transitions.²¹⁻²³ For example, the band density of states of Pd calculated by Mueller *et al.*²⁵ is shown in Fig. 6. The strength in the Pd density of states near

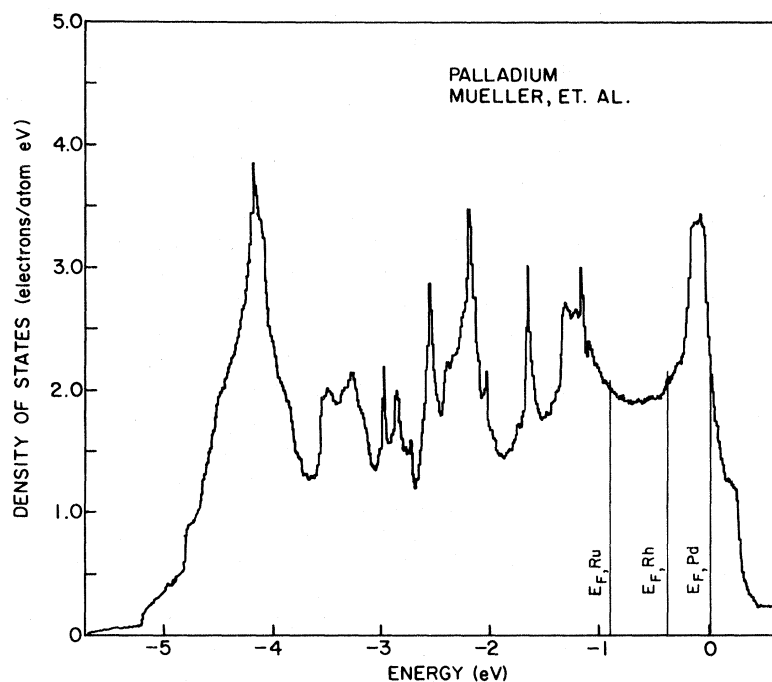


FIG. 6. Calculated density of states of Pd (Ref. 25) with the Fermi levels for Rh and Ru as determined by the rigid-band model.

the Fermi level is reflected in the strong structure near the Fermi level, i. e., the peak at -0.15 eV mentioned above in the Pd EDC's of Fig. 5. Likewise, the -1.2 -eV peak correlates with the peak in the density of states at about -1.2 eV. Judging from the Rh EDC's, similar strength near the Fermi level is expected in the Rh density of states. One might ask if a reasonable density of states for Rh can be obtained from the density of states of Pd (Fig. 6) using the simplest form of a rigid-band model in which the band structure and density of states for Rh is obtained by holding the Pd band structure fixed and shifting the Fermi level lower in energy so that there are nine instead of ten electrons per atom in filled states. In this model, the bandwidths are taken to be unchanged in going from Pd to Rh. The Rh density of states obtained in this way (Fig. 6 with the Rh Fermi level as shown) does not show the strength near the Fermi level expected

from the similarity between the Rh and Pd EDC's. Thus, our results appear to argue against this simple model. In this case x-ray photoemission measurements also show that such a simple rigid-band model is inadequate since the filled Rh bands are 0.3 eV²⁶ to 0.7 eV²⁷ wider than the corresponding Pd bands, whereas the simple model would predict bands narrower by about 0.4 eV. More experimental and theoretical work on this point is clearly justified; however, based on the presently available data, in our opinion, it does not appear that the simple rigid-band model is applicable for this system.

ACKNOWLEDGMENT

We would like to thank T. H. DiStefano for many helpful discussions, particularly concerning the energy analyzer.

[†]Work supported by the National Science Foundation and by the Advanced Research Projects Agency through the Center for Materials Research at Stanford University.

¹A. M. Clogston, G. T. Matthias, M. Peter, H. J. Williams, E. Corenzwit, and R. C. Sherwood, *Phys. Rev.* **125**, 541 (1962).

²J. T. Cox, G. Hass, and W. R. Hunter, *J. Opt. Soc. Am.* **61**, 360 (1971).

³G. Hass and R. Tousey, *J. Opt. Soc. Am.* **49**, 593 (1959).

⁴R. P. Madden and L. R. Canfield, *J. Opt. Soc. Am.* **51**, 838 (1961).

⁵D. W. Budworth, R. E. Hoare, and J. Preston, *Proc. Roy. Soc. (London)* **A257**, 250 (1960).

⁶F. E. Hoare and J. C. Matthews, *Proc. Roy. Soc. (London)* **212A**, 137 (1952).

⁷P. T. Coleridge, *Proc. Roy. Soc. (London)* **295**, 458 (1966).

⁸J. B. Ketterson, L. R. Windmiller, and S. Hörnfeldt, *Phys. Letters* **26A**, 115 (1968).

⁹O. K. Andersen, *Phys. Rev. B* **2**, 883 (1970).

¹⁰K. A. Kress and G. J. Lapeyre, *Phys. Rev. B* **2**, 2532 (1970).

¹¹J. F. Janak, D. E. Eastman, and A. R. Williams, *Solid State Commun.* **8**, 271 (1970).

¹²D. E. Eastman, *J. Appl. Phys.* **40**, 1387 (1969).

¹³T. H. DiStefano and D. T. Pierce, *Rev. Sci. Instr.* **41**, 180 (1970).

- ¹⁴D. T. Pierce and T. H. DiStefano, *Rev. Sci. Instr.* **41**, 1740 (1970).
¹⁵D. T. Pierce, Ph.D. dissertation (Stanford University, 1970) (unpublished).
¹⁶W. E. Spicer and C. N. Berglund, *Rev. Sci. Instr.* **35**, 1665 (1964).
¹⁷R. C. Eden, *Rev. Sci. Instr.* **41**, 252 (1970).
¹⁸N. V. Smith, *Phys. Rev. Letters* **23**, 1452 (1969).
¹⁹A. R. Williams, J. F. Janak, and V. L. Moruzzi (unpublished).
²⁰C. N. Berglund and W. E. Spicer, *Phys. Rev.* **136**, A1030 (1964); **136**, A1044 (1964).
²¹W. E. Spicer, *Phys. Rev.* **154**, 385 (1967).
²²R. K. Koyama and N. V. Smith, *Phys. Rev. B* **2**, 3049 (1970).
²³N. V. Smith, *Phys. Rev. B* **3**, 1862 (1971).
²⁴S. Doniach, *Phys. Rev. B* **2**, 3898 (1970).
²⁵F. M. Mueller, A. J. Freeman, J. O. Dimmock, and A. M. Furdyna, *Phys. Rev.* (to be published).
²⁶C. S. Fadley and D. A. Shirley, in *Proceedings of the Electronic Density of States Symposium*, National Bureau of Standards, Washington, D. C., 1969 (unpublished).
²⁷Y. Baer, P. F. Hedén, J. Hedman, M. Klasson, C. Nordling, and K. Siegbahn, *Physica Scripta* **1**, 55 (1970).

Elastic Constants of Dilute Mo-Re Alloys

K. M. Kesharwani and Bal K. Agrawal

Physics Department, University of Allahabad, Allahabad-2, India

(Received 14 September 1971)

The T -matrix method has been used for determining the effects of a low concentration of randomly distributed point defects on the elastic constants of a crystal of bcc structure. The expressions for the bulk elastic constants have been obtained in terms of the local changes in the central and noncentral force constants. The lattice dynamics of molybdenum have been discussed in Kreb's model with interactions up to second neighbors. The obtained eigenfrequencies and the eigenvectors are used to evaluate the different Green's-function matrix elements. Numerical estimates have been made for molybdenum crystal containing two different concentrations (7 and 7.4%) of rhenium. The results are compared with the experimentally measured elastic constants of the dilute alloys. An almost exact agreement between the theory and the experiment is observed.

I. INTRODUCTION

The elastic properties of a crystal containing a finite concentration of defects are significantly altered. The local strains around the defect are seen to be different from those of the host lattice. A knowledge of these strains, induced locally by the applied stress, is required to interpret a number of experimental measurements of the effects of elastic strains¹⁻⁴ and electric fields⁵ on the properties of crystals containing point defects. In recent years, some experiments have also been done to study the effect of defects on the bulk elastic properties of metals.⁶⁻⁸ Several theories^{9,10} have been proposed to account for these effects, but none of them takes into consideration the local behavior of defects and the discrete nature of the lattice. The T -matrix method takes into account, in a natural way, the peculiarities of the discrete nature of the lattice. A different theory has been developed by Ludwig¹¹ and Pistorious.¹² Earlier, the present authors applied a T -matrix method to determine the effect of substituted point defects on the elastic properties of the crystals of CsCl structure.^{13,14}

In the present paper, we use the T -matrix method

for determining the effects of a low concentration of randomly distributed point defects on the elastic properties of the crystals of bcc structure. Expressions for the bulk elastic constants have been obtained in terms of local changes of central and noncentral force constants in Sec. III. Numerical estimates have been made in Sec. IV for the case of molybdenum containing rhenium impurity ions. The calculated values are compared with the available experimental results.¹⁵

II. THEORY

Consider a solid containing a low concentration of similar substitutional point defects. In order to understand the lattice dynamics of the imperfect solid, one evaluates the perturbed phonon propagator as a Green's function which is given by

$$\underline{G}(z) = [\underline{L}_0 + \underline{P}_{sc}(\omega^2) - z\underline{I}]^{-1}, \quad (1)$$

where \underline{L}_0 is the mass-reduced dynamical matrix of the perfect host lattice and $\underline{P}_{sc}(\omega^2)$ is the perturbation matrix caused by a specific configuration of the defects. For the explicit forms of these matrices, we refer to an earlier paper.¹⁶ $z = \omega^2 + 2i\omega\xi^*$ is the complex squared frequency in the limit as $\xi^* \rightarrow 0^+$. The propagator defined by Eq. (1)